

On-the-Fly *Ab Initio* Hagedorn Wavepacket Dynamics: Single Vibronic Level Fluorescence Spectra of Difluorocarbene

Zhan Tong Zhang, Máté Visegrádi, and Jiří J. L. Vaníček*

Laboratory of Theoretical Physical Chemistry, Institut des Sciences et Ingénierie Chimiques,
Ecole Polytechnique Fédérale de Lausanne (EPFL), CH-1015 Lausanne, Switzerland

(Dated: December 17, 2024)

Hagedorn wavepackets have been used to compute single vibronic level (SVL) spectra efficiently in model harmonic potentials. To make the Hagedorn approach practical for realistic polyatomic molecules with anharmonicity, here we combine local harmonic Hagedorn wavepacket dynamics with on-the-fly *ab initio* dynamics. We then test this method by computing the SVL fluorescence spectra of difluorocarbene, a small, floppy molecule with a very anharmonic potential energy surface. Our time-dependent approach obtains the emission spectra of all initial vibrational levels from a single anharmonic semiclassical wavepacket trajectory without the need to fit individual anharmonic vibrational wavefunctions and to calculate the Franck–Condon factors for all vibronic transitions. We show that, whereas global harmonic models are inadequate for CF_2 , the spectra computed with the on-the-fly local harmonic Hagedorn wavepacket dynamics agree well with experimental data, especially for low initial excitations.

In the single vibronic level (SVL) fluorescence experiment, a molecule is first excited by a precise light source to a specific vibrational level in the electronic excited state, and its emission from that level is then measured. This emission spectrum provides information on the excited-state relaxation processes and on the higher vibrational levels of the ground electronic state [1–6].

Following Tapavicza’s generating function approach [7] and our derivation of algebraic expressions for the overlaps between any two Hagedorn functions [8], we recently developed a simple, time-dependent method for computing SVL spectra with Hagedorn wavepacket dynamics [9–11]. In this method, instead of individually evaluating the Franck–Condon overlaps for all vibronic transitions, the final spectrum is computed from the autocorrelation function between the initial wavepacket and the wavepacket propagated on the final electronic surface. This approach avoids the need to preselect the relevant transitions and can account for mode-mixing (Duschinsky rotation) and anharmonic effects more efficiently, avoiding the calculations of peaks that are not resolved in the experimental spectra. In addition, the Hagedorn approach has the advantage that a single Gaussian wavepacket trajectory is sufficient to compute the SVL emission spectra from any initial vibronic level.

Our approach was validated in harmonic model potentials [9], where the Hagedorn wavepackets are exact solutions to the time-dependent Schrödinger equation, and it was successfully applied to anthracene using a global harmonic model constructed from density functional theory calculations [10]. To investigate whether the Hagedorn method can capture moderate anharmonicity, we combined it with the local harmonic approximation (LHA) and, in a proof-of-principle study, demonstrated an improvement over global harmonic models in Morse systems for which exact quantum calculations were possible [11].

To make the method practical for real polyatomic

molecules, here we build on these preliminary results by combining the local harmonic Hagedorn wavepacket approach with on-the-fly *ab initio* semiclassical [12] dynamics [13–19]. Similar to the thawed Gaussian approximation [20, 21] used for evaluating ground-level emission and absorption spectra [22–26], the trajectory-based Hagedorn wavepacket dynamics avoids the need for precomputing a full anharmonic potential energy surface and instead relies on potential energy information evaluated locally during propagation. To test the on-the-fly Hagedorn approach on a realistic system, we compute the SVL spectra of difluorocarbene (CF_2), for which experimental results are available from the ground level up to the sixth excitation in the bending mode [27]. By extending the LHA to Hagedorn wavepacket dynamics, we aim to compute the emission from higher vibrational levels and simultaneously include the anharmonic effects without the need for variational or perturbative correction schemes.

In the Hagedorn wavepacket approach to SVL spectroscopy [9], the initial state $|K\rangle \equiv |e, K\rangle$ with vibrational quantum numbers $K = (K_1, \dots, K_D) \in \mathbb{N}_0^D$ in the electronic excited state e is represented in the excited-state normal-mode coordinates by the Hagedorn function [28, 29],

$$\varphi_K = (K!)^{-1/2} (A^\dagger)^K \varphi_0, \quad (1)$$

constructed from a D -dimensional, normalized, complex-valued Gaussian wavepacket (representing the ground vibrational wavefunction),

$$\begin{aligned} \varphi_0(q) = & \frac{1}{(\pi\hbar)^{D/4} \sqrt{\det(Q_t)}} \\ & \times \exp \left\{ \frac{i}{\hbar} \left[\frac{1}{2} x^T \cdot P_t \cdot Q_t^{-1} \cdot x + p_t^T \cdot x + S_t \right] \right\}, \quad (2) \end{aligned}$$

by applying the Hagedorn raising operator [30, 31],

$$A^\dagger := \frac{i}{\sqrt{2\hbar}} \left(P_t^\dagger \cdot (\hat{q} - q_t) - Q_t^\dagger \cdot (\hat{p} - p_t) \right). \quad (3)$$

In Eq. (1), $K! = K_1! \cdot K_2! \cdots K_D!$, and $(A^\dagger)^K = (A_1^\dagger)^{K_1} \cdot (A_2^\dagger)^{K_2} \cdots (A_D^\dagger)^{K_D}$, where A_j^\dagger is the j -th component of the raising operator A^\dagger . In Eq. (2), $x := q - q_t$ is the shifted position, and the Gaussian wavepacket φ_0 is parametrized by its “classical” position q_t and momentum p_t , two complex-valued D -dimensional matrices Q_t and P_t (such that $P_t \cdot Q_t^{-1}$ is the complex symmetric width matrix), and the classical action S_t . Matrices Q_t and P_t , related to the position and momentum covariances of the Gaussian [32], satisfy the so-called symplecticity conditions given by Eqs. (2.1) and (2.2) of Ref. [33], which ensure the commutation relations $[A_j, A_k] = [A_j^\dagger, A_k^\dagger] = 0$ and $[A_j, A_k^\dagger] = \delta_{jk}$ among Hagedorn’s raising operators A_j^\dagger and lowering operators A_k . Parametrization (2), originally proposed by Hagedorn [33, 34], facilitates the construction of Hagedorn functions (1) from Eqs. (2) and (3). These functions have the form of a Gaussian multiplied by a polynomial [30, 31] and are related to the generalized coherent states [35–39].

To meet the symplecticity conditions, we choose the initial parameters $Q_0 = (\text{Im } A_0)^{-1/2}$ and $P_0 = A_0 \cdot Q_0$, where A_0 is the width matrix of the ground vibrational Gaussian wavefunction in the excited electronic state. By propagating the initial vibrational wavepacket $|K\rangle = |\varphi_K\rangle$ on the electronic ground-state surface V_g , we obtain the autocorrelation function

$$C(t) = \langle \varphi_K | e^{-iH_g t/\hbar} | \varphi_K \rangle, \quad (4)$$

whose Fourier transform [7, 40, 41]

$$\sigma_{\text{em}}(\omega) = \frac{4\omega^3 |\mu_{ge}|^2}{3\pi\hbar c^3} \text{Re} \int_0^\infty \overline{C(t)} e^{it(\omega - \omega_{e,K})} dt \quad (5)$$

gives the rate of spontaneous emission from the vibrational level K in the excited electronic state e to the ground electronic state g as a function of frequency ω . In Eqs. (4) and (5), H_g is the ground-state Hamiltonian, μ_{ge} is the (constant) transition dipole moment within the Condon approximation, and $\hbar\omega_{e,K}$ is the vibronic energy of the initial state.

In the local harmonic approximation, the ground-state potential V_g is expanded at each time t around the current center q_t of the wavepacket as

$$V_{\text{LHA}}(q; q_t) := V(q_t) + V'(q_t) \cdot x + x^T \cdot V''(q_t) \cdot x/2. \quad (6)$$

Remarkably, Hagedorn wavepackets remain exact solutions to the time-dependent Schrödinger equation under this local harmonic potential V_{LHA} , with a set of partic-

ularly simple, classical-like equations,

$$\begin{aligned} \dot{q}_t &= m^{-1} \cdot p_t, & \dot{p}_t &= -V'(q_t) \\ \dot{Q}_t &= m^{-1} \cdot P_t, & \dot{P}_t &= -V''(q_t) \cdot Q_t, \\ \dot{S}_t &= L_t, \end{aligned} \quad (7)$$

where m is the mass matrix and L_t is the Lagrangian [31–33, 42]. These equations of motion are identical to those in the thawed Gaussian approximation, and the local harmonic propagation of the Hagedorn functions depends simply on the evolution of the Gaussian. Therefore, the SVL spectra from *all* vibrational levels may be computed “for free” from the *same* trajectory of the five parameters q_t, p_t, Q_t, P_t, S_t , needed already to evaluate the ground-level emission. The overlaps between the two Hagedorn wavepackets in the autocorrelation function (4) can be computed from the recurrence relations derived in Ref. [8]. The cost of these overlaps is negligible compared with the cost of *ab initio* calculations required to propagate the guiding Gaussian.

We assume that the initial wavepacket is a vibrationally excited state of a harmonic potential, which can be represented either by a single Hagedorn function (1) with a diagonal $Q_{0,jj} = (m_j \omega_j)^{-1/2}$ matrix or, equivalently, by the product

$$\varphi_K(q) = \langle q | K \rangle = \frac{\varphi_0(q)}{\sqrt{2^{|K|} |K|!}} \prod_{j=1}^D H_{K_j} \left(\sqrt{\frac{m\omega_j}{\hbar}} \cdot x_j \right) \quad (8)$$

of a Gaussian and D univariate Hermite polynomials [9, 31]. Here, we used the mass-weighted normal-mode coordinates of the initial, excited electronic surface, and ω_j is the angular frequency of the j -th vibrational mode with a common mass $m_j = m$. In general, however, Hagedorn functions are not simple products of one-dimensional Hermite functions [37, 43]. Under the effect of Duschinsky rotation, the excited-state vibrational eigenfunction will not remain separable if it is propagated with the ground-state potential. Yet, with the local harmonic Hagedorn wavepacket dynamics, the multi-index K of each Hagedorn function φ_K remains constant during the propagation of the parameters of the associated Gaussian.

The accuracy of the local harmonic dynamics of Hagedorn function φ_K depends on the anharmonicity of the potential V . Hagedorn [30] showed analytically that the L^2 -norm of the propagated wavefunction is of order $\mathcal{O}(\hbar^{1/2})$ under certain technical assumptions on the potential. In the one-dimensional case, he also proved that the error bound grows with the function’s excitation as $K^{3/2}$ and depends on $V'''(q)$. Alternatively, the accuracy of our approach can be studied numerically by simply comparing the local harmonic and exact quantum spectra; this was done for Morse-type model potentials in Ref. [11]. When the exact potential energy surface is known but exact quantum calculation is impractical, a

measure of accuracy may be derived by integrating the difference between the true and local harmonic Hamiltonians over time [31, 44] (thus estimating the “uncaptured” anharmonicity), similar to how the deviation vector is used to assess the variational dynamics of the Davydov ansatz [45].

To assess the accuracy of the local harmonic Hagedorn wavepacket dynamics in a realistic system, here we compute the emission spectra from the vibrational ground (2^0) level and the first six excited vibrational levels (2^1 to 2^6) in the bending mode (ν_2) of difluorocarbene (CF_2) and compare them to the experiments [27].

Difluorocarbene plays an important role in organic synthesis and is formed during plasma etching and chlorofluorocarbon decomposition processes [46–51]. With only three vibrational degrees of freedom, it also serves as a simple yet realistic model to test methods for simulating spectra beyond the global harmonic approximation.

Chau et al. [52] simulated the $\tilde{A}^1B_1 \rightarrow \tilde{X}^1A_1$ SVL spectra of CF_2 by fitting the potential energy function in a special form, variationally determining the anharmonic vibrational wavefunctions as a sum of products of one-dimensional harmonic oscillator eigenfunctions, and subsequently iteratively computing the Franck–Condon factors for each transition using the time-independent sum-over-states expression of vibronic spectroscopy.

In our time-dependent method, the local harmonic SVL spectra were evaluated from a single anharmonic on-the-fly wavepacket trajectory, obtained by evaluating the potential energy V , gradient V' , and Hessian V'' locally at each time step and propagating the wavepacket according to Eqs. (7). All electronic structure calculations were performed with Gaussian 16 [53] at the PBE0/aug-cc-pVTZ level of theory [54, 55]. See the Supplemental Material for the optimized geometries and frequencies of CF_2 in the ground and first excited singlet states compared to the experimental data.

To investigate the importance of anharmonicity, we simulated the 2^0 and 2^2 spectra also using Hagedorn dynamics combined with one of two global harmonic approximations [9, 10]. The adiabatic harmonic model employs the expansion

$$V_{\text{AHA}}(q) = V_g(q_{\text{eq},g}) + (q - q_{\text{eq},g})^T \cdot V_g''(q_{\text{ref},g}) \cdot (q - q_{\text{eq},g}) / 2 \quad (9)$$

of the potential V_g around the optimized ground-state equilibrium geometry $q_{\text{eq},g}$, whereas the vertical harmonic model employs the expansion

$$V_{\text{VHA}}(q) = V_g(q_{\text{eq},e}) + V_g'(q_{\text{eq},e})^T \cdot (q - q_{\text{eq},e}) + (q - q_{\text{eq},e})^T \cdot V_g''(q_{\text{eq},e}) \cdot (q - q_{\text{eq},e}) / 2 \quad (10)$$

of the potential around the Franck–Condon point, that is, the optimized excited-state equilibrium geometry $q_{\text{eq},e}$.

In both the local and global harmonic simulations, the parameters of the Gaussian were propagated for a total

time of 16000 a.u. (~ 387 fs) using the second-order TVT geometric integrator [32, 42] based on the Strang splitting [56]. A small time step of 8 a.u. was used to ensure the accuracy of the dynamics. For each initial vibrational level, the autocorrelation function was computed every two steps. As the spectrum (5) is the Fourier transform of the autocorrelation function, calculating the wavepacket overlaps less frequently (i.e., at every other step) reduces only the spectral range, which remains sufficient to cover the relevant part of the spectra in our case (see Figs. 1 and 2). The overlaps between the Hagedorn wavepackets were evaluated using the algebraic algorithm derived in Ref. [8] (see Eqs. 97 and 98 therein) and the publicly available code from Ref. [9]. A Gaussian damping function was applied to the autocorrelation functions such that the spectral peaks were broadened by a Gaussian with a half-width at half-maximum of 50 cm^{-1} .

Figure 1 compares the emission spectra from vibrational levels 2^0 and 2^2 computed using the local and global harmonic models with the experimental spectra. The wavenumbers of experimental spectra were shifted such that the transition to the vibrational ground level in each spectrum was at 0 cm^{-1} . In other words, the intensity is plotted as a function of the difference $\Delta\tilde{\nu} = \tilde{\nu}_{\text{em}} - \tilde{\nu}_{\text{exc}}$ between the wavenumbers of the emitted light and of the initial excitation light; the peaks at more negative wavenumbers correspond to transitions to higher vibrational levels in the ground electronic state. Before the ω^3 scaling factor in Eq. (5) was applied, each computed spectrum was horizontally shifted to remove the relatively large error in the electronic excitation energy provided by the electronic structure program (see the Supplementary Material for details). To facilitate the comparison, we scaled both the computed and experimental spectra by setting the intensity of the highest peak in each spectrum to unity.

In the ground-level spectrum (2^0 , first row), the adiabatic harmonic model describes the peaks closer to 0 cm^{-1} reasonably well and provides the correct spacing between the peaks. However, it significantly overestimates the intensity of the transitions to the higher vibrational levels ($\Delta\tilde{\nu} < -5000 \text{ cm}^{-1}$) in the ground state. The vertical harmonic model captures the overall envelope of the spectra quite well but yields a poorly resolved spectrum with a broad tail at more negative values of $\Delta\tilde{\nu}$.

The delocalization of the wavepacket increases with the initial vibrational excitation and amplifies the effects of anharmonicity. Although the adiabatic model qualitatively captures the splitting of the envelope in the 2^2 spectrum (second row), the splitting positions and the intensity patterns are incorrect. The spectrum of the vertical harmonic model also exhibits splitting of the envelope and arguably captures it better than the adiabatic model, but the resolution remains poor at lower wavenumbers.

In contrast to the global harmonic models, the local

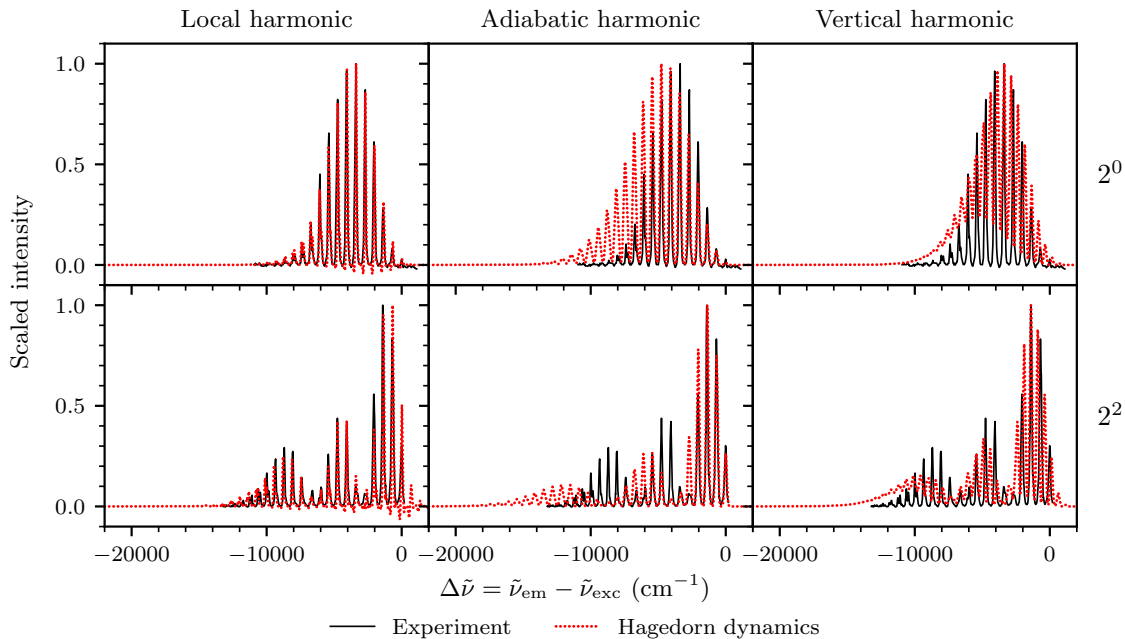


FIG. 1. Comparison of the experimental (black solid line) SVL fluorescence spectra from 2^0 and 2^2 levels of CF_2 from Ref. [27] with computed (red dotted line) spectra using the local, adiabatic, and vertical harmonic Hagedorn wavepacket dynamics; the intensity is plotted as a function of the difference $\Delta\tilde{\nu} = \tilde{\nu}_{\text{em}} - \tilde{\nu}_{\text{exc}}$ between the wavenumbers of the emitted photon and of the light used for the initial vibronic excitation.

harmonic dynamics (first column of Fig. 1) reproduces remarkably well the experimental peak positions and intensities in both 2^0 and 2^2 spectra. In the 2^2 case (second row), the local harmonic spectrum predicts correctly the locations of the envelope splitting. The significant improvement observed with the local harmonic Hagedorn wavepacket dynamics highlights the importance of including anharmonic effects in the SVL spectra of small, floppy molecules, particularly with a higher initial excitation, even when the ground-level spectrum computed with global harmonic models is satisfactory.

Next, we employed the same on-the-fly *ab initio* trajectory that we had used for the 2^0 and 2^2 spectra to compute the emission spectra of CF_2 also from levels $2^1, 2^3, 2^4, 2^5$ and 2^6 . Each of these SVL spectra is dominated by the bending-mode (mode 2) progression, whose envelope is split according to the initial vibrational excitation [27]. To facilitate the comparison of the computed and experimental spectra in Fig. 2, we applied artificial broadening to the experimental values [27] of the wavelengths and spectral intensities of the emission peaks from 2^0 to 2^6 levels.

In Fig. 2, the local harmonic spectra deviate more from the experimental ones as the initial vibrational excitation increases. However, the local harmonic dynamics still captures the correct splitting pattern due to the vibrational excitation of the initial state and yields reasonable peak spacing and intensities for $\Delta\tilde{\nu} > -5000 \text{ cm}^{-1}$ even

with relatively high initial vibrational excitations.

Although the same *ab initio* trajectory is used, the performance of our approach becomes poorer for spectra with higher initial vibrational excitations, which is in agreement with Hagedorn’s error bound [30]. Even if the initial, excited-state surface is completely harmonic, an initial nuclear wavepacket with higher vibrational excitation becomes more delocalized and, when propagated on the anharmonic ground-state surface, is exposed to stronger anharmonic effects in regions farther from the wavepacket’s center, where the local harmonic approximation becomes insufficient. In addition, the assumption of a harmonic excited-state surface, which justifies representing the initial wavepacket by a single Hagedorn function, may break down as the initial vibrational excitation increases.

Nonetheless, the local harmonic Hagedorn wavepacket approach is suitable for evaluating SVL spectra with relatively low excitations, and its on-the-fly implementation is very efficient. The emission spectra from all vibrational levels are obtained from a single trajectory without the need to rerun expensive electronic structure calculations for different initial states. This advantage becomes even more important in higher-dimensional systems containing more atoms and electrons. Additionally, the local harmonic approach may potentially perform better in larger molecules that are less floppy and hence less anharmonic than CF_2 .

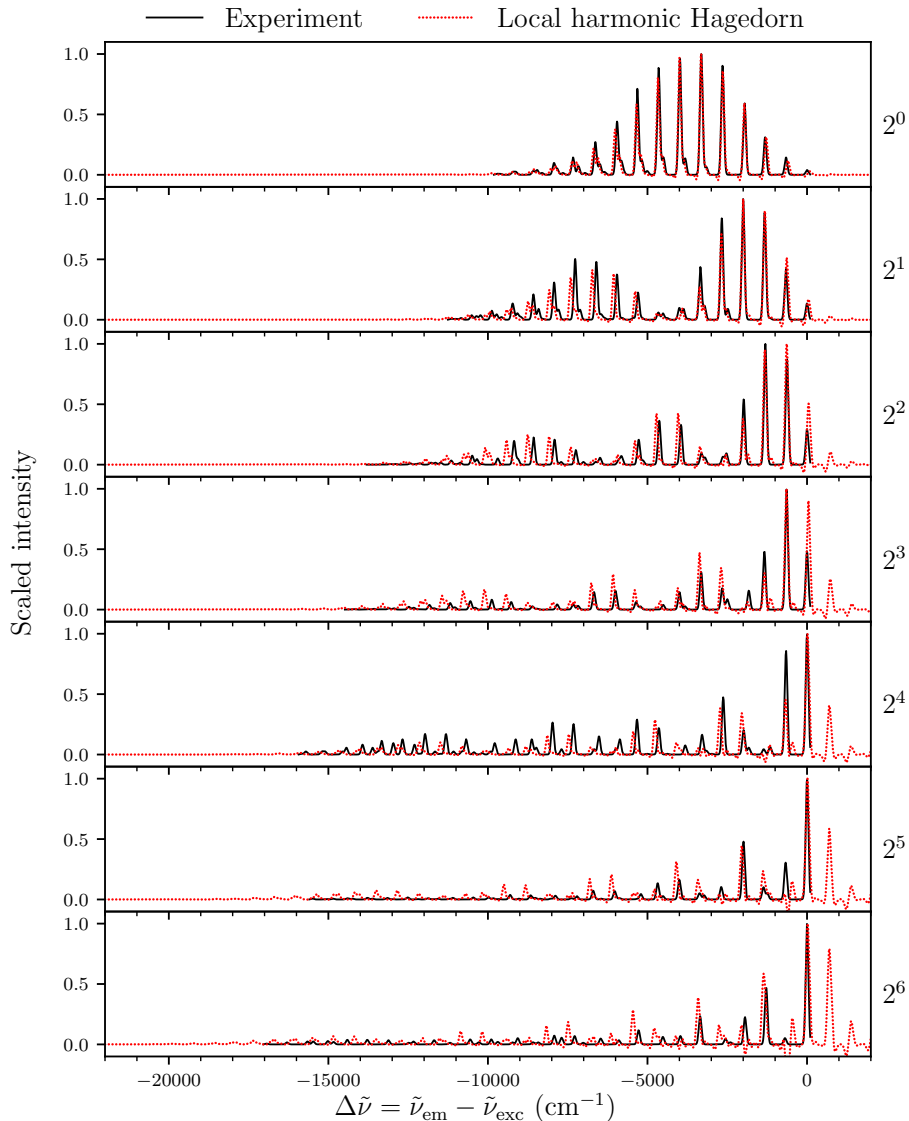


FIG. 2. Comparison of computed (red dotted line) and experimental (black solid line) fluorescence spectra of CF_2 from 2^0 to 2^6 levels, plotted as a function of the difference $\Delta\tilde{\nu} = \tilde{\nu}_{\text{em}} - \tilde{\nu}_{\text{exc}}$ between the wavenumbers of the emitted photon and of the initial excitation light; the experimental spectra are artificially broadened based on wavelength and intensity values from Table I of Ref. [27].

Alternative approaches employing time-dependent bases, such as the multiconfigurational time-dependent Hartree method [57, 58], multiple spawning [59], coupled coherent states [60], variational multiconfigurational Gaussians [61], Gauss–Hermite basis [62, 63], and multiple Davydov ansatz [45, 64, 65], have been used to obtain highly accurate results for molecular quantum dynamics. Similarly, our approach can be made more accurate by expanding the wavepacket as a linear combination of multiple Hagedorn functions (associated with the same guiding Gaussian) and propagating the expansion coefficients using the time-dependent variational principle [31, 33]. Such variational approach has been applied

to several model problems [33, 66–68], and its errors and other properties have been rigorously studied by mathematicians [31, 34, 42, 69–71].

Our local harmonic Hagedorn approach, however, offers a quick and straightforward way to incorporate anharmonic effects in vibronic spectra arising from vibrationally excited states, using almost the same mathematical machinery as in the global harmonic case [9, 10]. In contrast, the more accurate variational Hagedorn method requires a separate, variational propagation of the coefficients for each initial excitation and, as dimensions grow, an increasing number of basis functions. An on-the-fly variational implementation would also require ef-

ficient electronic structure methods capable of providing accurate third- or higher-order derivatives.

In conclusion, we successfully combined the local harmonic Hagedorn wavepacket approach with on-the-fly *ab initio* molecular dynamics to simulate the SVL fluorescence spectra of polyatomic molecules. Using a single semiclassical wavepacket trajectory, we were able to evaluate SVL emission spectra from different initial vibronic levels of the small and flexible CF₂ molecule. Whereas the global harmonic models proved to be inadequate for CF₂, the local harmonic Hagedorn method resulted in good agreement with the experimental data, at least for lower initial vibrational excitations. Propagation with the local harmonic approximation requires potential energy surface information evaluated only at a single molecular geometry at each time step, and obtaining SVL emission spectra from arbitrary initial vibrational levels incurs minimal additional computational expenses with Hagedorn dynamics. Thus, our efficient method can be applied to larger molecules, similar to how the thawed Gaussian approximation has been used for emission and absorption spectra from the ground vibrational level [23, 72, 73]. Finally, the on-the-fly local harmonic Hagedorn wavepacket approach should be applicable to other vibronic spectroscopy techniques involving excited vibrational states [74–79] and to more situations with non-Gaussian initial states [80, 81], such as the computation of Herzberg–Teller spectra [82–85] and internal conversion rates [86].

The authors acknowledge financial support from the EPFL.

* jiri.vanicek@epfl.ch

- [1] E. W. Schlag and H. v. Weyssenhoff, *J. Chem. Phys.* **51**, 2508 (1969).
- [2] C. Parmenter and M. Schuyler, in *Transitions non radiatives dans les molécules : 20e réunion de la Société de chimie physique, Paris, 27 au 30 mai 1969* (Société de chimie physique, 1970) p. 92.
- [3] P. M. Felker and A. H. Zewail, *J. Chem. Phys.* **82**, 2975 (1985).
- [4] M. Quack and M. Stockburger, *J. Mol. Spec.* **43**, 87 (1972).
- [5] T. C. Smith, M. Gharaibeh, and D. J. Clouthier, *J. Chem. Phys.* **157**, 204306 (2022).
- [6] R. Suzuki, K. Chiba, S. Tanaka, and K. Okuyama, *J. Chem. Phys.* **160**, 024301 (2024).
- [7] E. Tapavicza, *J. Phys. Chem. Lett.* **10**, 6003 (2019).
- [8] J. J. L. Vaníček and Z. T. Zhang, On Hagedorn wavepackets associated with different Gaussians (2024), arXiv:2405.07880 [quant-ph].
- [9] Z. T. Zhang and J. J. L. Vaníček, *J. Chem. Phys.* **161**, 111101 (2024).
- [10] Z. T. Zhang and J. J. L. Vaníček, Ab initio simulation of single vibronic level fluorescence spectra of anthracene using Hagedorn wavepackets (2024), arXiv:2403.00702 [physics.chem-ph].
- [11] Z. T. Zhang, M. Visegrádi, and J. J. L. Vaníček, Capturing anharmonic effects in single vibronic level fluorescence spectra using local harmonic Hagedorn wavepacket dynamics (2024), arXiv:2408.11991 [physics.chem-ph].
- [12] W. H. Miller, *J. Phys. Chem. A* **105**, 2942 (2001).
- [13] J. Tatchen and E. Pollak, *J. Chem. Phys.* **130**, 041103 (2009).
- [14] M. Ceotto, S. Atahan, S. Shim, G. F. Tantardini, and A. Aspuru-Guzik, *Phys. Chem. Chem. Phys.* **11**, 3861 (2009).
- [15] S. Y. Y. Wong, D. M. Benoit, M. Lewerenz, A. Brown, and P.-N. Roy, *J. Chem. Phys.* **134**, 094110 (2011).
- [16] K. Saita and D. V. Shalashilin, *J. Chem. Phys.* **137**, 22A506 (2012).
- [17] M. Ceotto, G. Di Liberto, and R. Conte, *Phys. Rev. Lett.* **119**, 010401 (2017).
- [18] G. Di Liberto, R. Conte, and M. Ceotto, *J. Chem. Phys.* **148**, 104302 (2018).
- [19] S. V. Pios, M. F. Gelin, L. Vasquez, J. Hauer, and L. Chen, *J. Phys. Chem. Lett.* **15**, 8728 (2024).
- [20] E. J. Heller, *J. Chem. Phys.* **62**, 1544 (1975).
- [21] E. J. Heller, *The Semiclassical Way to Dynamics and Spectroscopy* (Princeton University Press, Princeton, NJ, 2018).
- [22] M. Wehrle, M. Šulc, and J. Vaníček, *J. Chem. Phys.* **140**, 244114 (2014).
- [23] M. Wehrle, S. Oberli, and J. Vaníček, *J. Phys. Chem. A* **119**, 5685 (2015).
- [24] T. Begušić, E. Tapavicza, and J. Vaníček, *J. Chem. Theory Comput.* **18**, 3065 (2022).
- [25] E. Klėtnieks, Y. C. Alonso, and J. J. L. Vaníček, *J. Phys. Chem. A* **127**, 8117 (2023).
- [26] R. Gherib, I. G. Ryabinkin, and S. N. Genin, Thawed Gaussian wavepacket dynamics with Δ -machine learned potentials (2024), arXiv:2405.00193 [physics.chem-ph].
- [27] D. S. King, P. K. Schenck, and J. C. Stephenson, *J. Mol. Spec.* **78**, 1 (1979).
- [28] G. A. Hagedorn, *Ann. Phys. (NY)* **135**, 58 (1981).
- [29] G. A. Hagedorn, *Ann. Henri Poincaré* **42**, 363 (1985).
- [30] G. A. Hagedorn, *Ann. Phys. (NY)* **269**, 77 (1998).
- [31] C. Lasser and C. Lubich, *Acta Numerica* **29**, 229 (2020).
- [32] J. J. L. Vaníček, *J. Chem. Phys.* **159**, 014114 (2023).
- [33] E. Faou, V. Gradinaru, and C. Lubich, *SIAM J. Sci. Comp.* **31**, 3027 (2009).
- [34] G. A. Hagedorn, *Commun. Math. Phys.* **71**, 77 (1980).
- [35] M. Combescure, *J. Math. Phys.* **33**, 3870 (1992).
- [36] M. Combescure and D. Robert, *Coherent States and Applications in Mathematical Physics*, Theoretical and Mathematical Physics Ser. (Springer Netherlands, Dordrecht, 2012).
- [37] C. Lasser and S. Troppmann, *J. Fourier Anal. Appl.* **20**, 679 (2014).
- [38] R. Borrelli and M. F. Gelin, *Chem. Phys.* **481**, 91 (2016).
- [39] L. Chen, R. Borrelli, and Y. Zhao, *J. Phys. Chem. A* **121**, 8757–8770 (2017).
- [40] E. J. Heller, *Acc. Chem. Res.* **14**, 368 (1981).
- [41] D. J. Tannor, *Introduction to Quantum Mechanics: A Time-Dependent Perspective* (University Science Books, Sausalito, 2007).
- [42] C. Lubich, *From Quantum to Classical Molecular Dynamics: Reduced Models and Numerical Analysis* (European Mathematical Society, Zürich, 2008).
- [43] T. Ohsawa, *J. Fourier Anal. Appl.* **25**, 1513 (2019).

- [44] S. Burkhard, B. Dörich, M. Hochbruck, and C. Lasser, *J. Phys. A* **57**, 295202 (2024).
- [45] Y. Zhao, K. Sun, L. Chen, and M. Gelin, *WIREs Comput. Mol. Sci.* **12**, e1589 (2022).
- [46] X. Ma, J. Su, and Q. Song, *Acc. Chem. Res.* **56**, 592 (2023).
- [47] Q. Xie and J. Hu, *Acc. Chem. Res.* **57**, 693 (2024).
- [48] N. Bulcourt, J.-P. Booth, E. A. Hudson, J. Luque, D. K. W. Mok, E. P. Lee, F.-T. Chau, and J. M. Dyke, *J. Chem. Phys.* **120**, 9499 (2004).
- [49] M. F. Cuddy and E. R. Fisher, *ACS Appl. Mater. Interfaces* **4**, 1733 (2012).
- [50] R. E. Rebbert and P. J. Ausloos, *J. Photochem.* **4**, 419 (1975).
- [51] N. Sonoyama, K. Ezaki, H. Fujii, and T. Sakata, *Electrochim. Acta* **47**, 3847 (2002).
- [52] F.-T. Chau, J. M. Dyke, E. P. F. Lee, and D. K. W. Mok, *J. Chem. Phys.* **115**, 5816 (2001).
- [53] M. J. Frisch, G. W. Trucks, H. B. Schlegel, G. E. Scuseria, M. A. Robb, J. R. Cheeseman, G. Scalmani, V. Barone, G. A. Petersson, H. Nakatsuji, X. Li, M. Caricato, A. V. Marenich, J. Bloino, B. G. Janesko, R. Gomperts, B. Mennucci, H. P. Hratchian, J. V. Ortiz, A. F. Izmaylov, J. L. Sonnenberg, D. Williams-Young, F. Ding, F. Lipparini, F. Egidi, J. Goings, B. Peng, A. Petrone, T. Henderson, D. Ranasinghe, V. G. Zakrzewski, J. Gao, N. Rega, G. Zheng, W. Liang, M. Hada, M. Ehara, K. Toyota, R. Fukuda, J. Hasegawa, M. Ishida, T. Nakajima, Y. Honda, O. Kitao, H. Nakai, T. Vreven, K. Throssell, J. A. Montgomery, Jr., J. E. Peralta, F. Ogliaro, M. J. Bearpark, J. J. Heyd, E. N. Brothers, K. N. Kudin, V. N. Staroverov, T. A. Keith, R. Kobayashi, J. Normand, K. Raghavachari, A. P. Rendell, J. C. Burant, S. S. Iyengar, J. Tomasi, M. Cossi, J. M. Millam, M. Klene, C. Adamo, R. Cammi, J. W. Ochterski, R. L. Martin, K. Morokuma, O. Farkas, J. B. Foresman, and D. J. Fox, *Gaussian 16 Revision C.01* (2016), Gaussian Inc. Wallingford CT.
- [54] C. Adamo and V. Barone, *J. Chem. Phys.* **110**, 6158 (1999).
- [55] R. A. Kendall, T. H. Dunning, and R. J. Harrison, *J. Chem. Phys.* **96**, 6796 (1992).
- [56] E. Hairer, C. Lubich, and G. Wanner, *Geometric Numerical Integration: Structure-Preserving Algorithms for Ordinary Differential Equations* (Springer Berlin Heidelberg New York, 2006).
- [57] H.-D. Meyer, U. Manthe, and L. S. Cederbaum, *Chem. Phys. Lett.* **165**, 73 (1990).
- [58] M. Beck, A. Jäckle, G. Worth, and H.-D. Meyer, *Phys. Rep.* **324**, 1 (2000).
- [59] M. Ben-Nun, J. Quenneville, and T. J. Martínez, *J. Phys. Chem. A* **104**, 5161 (2000).
- [60] D. V. Shalashilin and M. S. Child, *Chem. Phys.* **304**, 103 (2004).
- [61] G. A. Worth, M. A. Robb, and I. Burghardt, *Faraday Discuss.* **127**, 307 (2004).
- [62] S. Adhikari and G. D. Billing, *Chem. Phys.* **238**, 69 (1998).
- [63] G. D. Billing, *Phys. Chem. Chem. Phys.* **4**, 2865 (2002).
- [64] N. Zhou, Z. Huang, J. Zhu, V. Chernyak, and Y. Zhao, *J. Chem. Phys.* **143**, 014113 (2015).
- [65] Y. Zhao, *J. Chem. Phys.* **158**, 080901 (2023).
- [66] E. Kieri, S. Holmgren, and H. O. Karlsson, *J. Chem. Phys.* **137**, 044111 (2012).
- [67] Z. Zhou, *J. Comput. Phys.* **272**, 386 (2014).
- [68] V. Gradinaru and O. Rietmann, *J. Comput. Phys.* **445**, 110581 (2021).
- [69] G. Hagedorn and A. Joye, *Ann. Henri Poincaré* **1**, 837 (2000).
- [70] V. Gradinaru and G. A. Hagedorn, *Numer. Math.* **126**, 53 (2014).
- [71] T. Ohsawa, *Nonlinearity* **31**, 1807 (2018).
- [72] T. Begušić, M. Cordova, and J. Vaníček, *J. Chem. Phys.* **150**, 154117 (2019).
- [73] T. Begušić and J. Vaníček, *J. Chem. Phys.* **153**, 024105 (2020).
- [74] L. J. G. W. van Wilderen, A. T. Messmer, and J. Bredenbeck, *Angew. Chem. Int. Ed.* **53**, 2667 (2014).
- [75] H. Yu, N. L. Evans, A. S. Chatterley, G. M. Roberts, V. G. Stavros, and S. Ullrich, *J. Phys. Chem. A* **118**, 9438 (2014).
- [76] A. Baiardi, J. Bloino, and V. Barone, *J. Chem. Phys.* **141**, 114108 (2014).
- [77] L. Whaley-Mayda, A. Guha, S. B. Penwell, and A. Tokmakoff, *J. Am. Chem. Soc.* **143**, 3060 (2021).
- [78] J. A. Lau, M. DeWitt, M. A. Boyer, M. C. Babin, T. Solomis, M. Grellmann, K. R. Asmis, A. B. McCoy, and D. M. Neumark, *J. Phys. Chem. A* **127**, 3133 (2023).
- [79] M. Horz, H. M. A. Masood, H. Brunst, J. Cerezo, D. Picconi, H. Vormann, M. S. Niraghatam, L. J. G. W. Van Wilderen, J. Bredenbeck, F. Santoro, and I. Burghardt, *J. Chem. Phys.* **158**, 064201 (2023).
- [80] S.-Y. Lee and E. J. Heller, *J. Chem. Phys.* **76**, 3035 (1982).
- [81] D. J. Tannor and E. J. Heller, *J. Chem. Phys.* **77**, 202 (1982).
- [82] A. Baiardi, J. Bloino, and V. Barone, *J. Chem. Theory Comput.* **9**, 4097 (2013).
- [83] M. Bonfanti, J. Petersen, P. Eisenbrandt, I. Burghardt, and E. Pollak, *J. Chem. Theory Comput.* **14**, 5310 (2018).
- [84] A. Patoz, T. Begušić, and J. Vaníček, *J. Phys. Chem. Lett.* **9**, 2367 (2018).
- [85] S. Kundu, P. P. Roy, G. R. Fleming, and N. Makri, *J. Phys. Chem. B* **126**, 2899 (2022).
- [86] M. Wenzel and R. Mitric, *J. Chem. Phys.* **158**, 034105 (2023).

Supplemental Material to On-the-Fly *Ab Initio* Hagedorn Wavepacket Dynamics: Single Vibronic Level Fluorescence Spectra of Difluorocarbene

Zhan Tong Zhang, Máté Visegrádi, and Jiří Vaníček

Laboratory of Theoretical Physical Chemistry,

Institut des Sciences et Ingénierie Chimiques,

Ecole Polytechnique Fédérale de Lausanne (EPFL), CH-1015 Lausanne, Switzerland

I. OPTIMIZED GEOMETRIES AND FREQUENCIES OF THE \tilde{X}^1A_1 AND \tilde{A}^1B_1 STATES OF CF_2

The equilibrium geometries (r : C-F bond length; θ : C-F-C bond angle) of the ground \tilde{X}^1A_1 and first excited \tilde{A}^1B_1 electronic states and the corresponding vibrational frequencies were calculated using the PBE0 functional and the aug-cc-pVTZ basis set. The computed values are compared to the experimental data [1–3] (as summarized in Ref. [4]) in Table I.

\tilde{X}^1A_1	$r/\text{\AA}$	θ/deg	ω_1/cm^{-1}	ω_2/cm^{-1}	ω_3/cm^{-1}
PBE0/aug-cc-pVTZ	1.2965	104.77	1255.43	680.61	1151.23
Expt	1.2975	104.81	1275.08	666.25	1114.44

(a) Ground electronic state

\tilde{A}^1B_1	$r/\text{\AA}$	θ/deg	ω_1/cm^{-1}	ω_2/cm^{-1}	ω_3/cm^{-1}
TD-PBE0/aug-cc-pVTZ	1.3054	123.27	1109.14	500.84	1362.81
Expt	1.316	122.3	1011	496	1180

(b) Excited electronic state

TABLE I: Geometries of CF_2 optimized at PBE0/aug-cc-pVTZ level of theory and the fundamental vibrational frequencies; for comparison, the experimentally (Expt) derived values are also shown.

II. PROCEDURE USED TO SHIFT AND SCALE THE SVL EMISSION SPECTRA

Because the error in the electronic excitation energy obtained from electronic structure calculations is larger than the vibrational spacing in the spectra, a horizontal shift is applied to the computed spectra. Determining this shift correctly is crucial because the shift fixes the “zero” of frequency and therefore affects the frequency-dependent ω^3 factor in Eq. (5), which is applied to the “wavepacket” spectra obtained by the Fourier transform of the autocorrelation function.

For each initial vibrational level K of the excited electronic state, we applied the following procedure to the computed SVL fluorescence spectrum:

Step 1: The computed spectrum is horizontally shifted to account for the error in the electronic excitation energy obtained from electronic structure calculations. This shift determines the $\tilde{\nu}_{\text{em}}$ of the computed spectrum.

— In the adiabatic harmonic model, where the 2_0^K transition (i.e., the transition to the vibrational ground level of the electronic ground state) is well-defined and clearly visible, the computed spectrum is shifted such that its 2_0^K peak aligns with the 2_0^K peak in the experimental spectrum.

— In the vertical and local harmonic cases, the computed spectrum is shifted such that its highest peak aligns with the highest peak in the experimental spectrum. Note: When multiple SVL spectra are obtained from the same ab initio trajectory, their shifts should be approximately the same. In particular, the differences between the shifts should be much smaller than the vibrational spacing between the peaks. If a shift for one SVL differs substantially from others, the alignment for that SVL should be adjusted by the vibrational spacing. See below for an example in the local harmonic 2^2 spectrum of CF_2 .

Step 2: The spectrum computed by a Fourier transform of the autocorrelation function is multiplied by $\tilde{\nu}_{\text{em}}^3$ (since $\tilde{\nu}_{\text{em}} \propto \omega$ and the intensities will be normalized in the next step).

— In the vertical and local harmonic cases only, one needs to check the following: If, after applying the $\tilde{\nu}_{\text{em}}^3$ factor, the highest peak in the computed spectrum changes, the horizontal shift is revised such that the highest peak (after multiplication) is aligned to the highest experimental peak and Step 2 is repeated until the spectrum scaled by $\tilde{\nu}_{\text{em}}^3$ converges.

Step 3: The intensity of the highest peak is set to 1 in both computed and experimental spectra.

A. Example of the adjustment in Step 1

In the 2^2 local harmonic spectra of CF_2 (see Figs. 1 and 2 of the main text), the two highest peaks are neighboring each other and have similar intensities. The shift determined by matching the highest peaks produced a spectrum that appeared to be one vibrational quantum off from the experimental reference. This situation can be detected automatically and rigorously by a general procedure, which we demonstrate on our example of 2^2 local harmonic spectra of CF_2 :

We noticed that the shift determined in Step 1 for the 2^2 spectrum was quite different (by approximately one vibrational quantum, $\sim 650 \text{ cm}^{-1}$) from the shifts determined for other spectra obtained from the same trajectory:

Initial vibrational excitation	Difference from average shift (determined by highest peak) (cm^{-1})
2^0	-170
2^1	-125
2^2	553
2^3	-105
2^4	-65
2^5	-50
2^6	-40

We thus decided to shift the highest peak of the computed 2^2 spectrum to align with the second-highest peak in the experiment. The shifts for all spectra are consistent after this adjustment:

Initial vibrational excitation	Difference from average shift (determined by highest peak) (cm^{-1})
2^0	-74
2^1	-29
2^2	-24
2^3	-9
2^4	31
2^5	46
2^6	56

This suggests that the alignments of all SVL spectra are correct and, indeed, the computed

2^2 spectrum now matches the experimental one better.

- [1] F. Comes and D. Ramsay, *J. Mol. Spec.* **113**, 495 (1985).
- [2] M. R. Cameron, S. H. Kable, and G. B. Bacskay, *J. Chem. Phys.* **103**, 4476 (1995).
- [3] L. Margulès, J. Demaison, and J. E. Boggs, *J. Phys. Chem. A* **103**, 7632 (1999).
- [4] F.-T. Chau, J. M. Dyke, E. P. F. Lee, and D. K. W. Mok, *J. Chem. Phys.* **115**, 5816 (2001).